

Thermal analysis of metastable Fe-Cu-Ag prepared by mechanical alloying

This article has been downloaded from IOPscience. Please scroll down to see the full text article.

1998 J. Phys.: Condens. Matter 10 1665

(<http://iopscience.iop.org/0953-8984/10/7/014>)

View [the table of contents for this issue](#), or go to the [journal homepage](#) for more

Download details:

IP Address: 171.66.16.209

The article was downloaded on 14/05/2010 at 12:18

Please note that [terms and conditions apply](#).

Thermal analysis of metastable Fe–Cu–Ag prepared by mechanical alloying

Q A Pankhurst[†], N S Cohen[†] and M Odlyha[‡]

[†] Department of Physics and Astronomy, University College London, Gower Street, London WC1E 6BT, UK

[‡] Department of Chemistry, Birkbeck College, London WC1H 0PP, UK

Received 23 October 1997, in final form 14 November 1997

Abstract. The thermal properties of metastable Fe–Cu–Ag alloys have been investigated using differential scanning calorimetry, complementing an earlier x-ray diffraction and Mössbauer spectroscopy study. Samples were mechanically alloyed under nitrogen in a high-energy ball mill for 70 hours. DSC and x-ray data on milled and unmilled elemental powders show that Fe sustains more lattice distortion than Cu or Ag, with an rms strain of order 0.6%. In the equimolar binary alloys Fe–Cu, Fe–Ag and Cu–Ag the presence of DSC exotherms below 400 °C is found to correspond to a gradual decomposition of the alloy, while exotherms above 400 °C denote recrystallization and grain growth. The absence of low-temperature DSC exotherms in Fe–Ag confirms phase segregation in this granular alloy. In equimolar Fe–Cu–Ag, DSC curves after successive heat treatments indicate a highly disordered state, with fine-scale residual crystallinity. Heating promotes the decomposition of this metastable state into polycrystalline and segregated Fe, Cu and Ag.

1. Introduction

The metals Fe, Cu and Ag are naturally immiscible, but through prolonged and energetic ball milling (70 hours at 600 rpm) it is possible to produce metastable alloys, the structure of which depends on elemental composition. These alloys are of both fundamental and applied interest. The fundamental interest lies in the nature of the metastable states that may be accessed through mechanical alloying, that are not otherwise attainable. Of special interest is the central portion of the ternary Fe–Cu–Ag phase diagram, where amorphous phases have been found in sputter-deposited thin films [1, 2]. The primary question is whether this amorphous state, or some analogous state, can be accessed by mechanical means, and if so, what its characteristics are. The applied interest stems from the fact that granular Fe–Ag binary alloys exhibit giant magnetoresistance, where the electrical resistivity of the alloy can be markedly changed by the application of a magnetic field [3, 4]. These materials have potential application in magnetic sensors and switches. The main question here is whether the addition of Cu to the Fe–Ag system might be a means of controlling its microstructure in a way that enhances its magnetoresistive properties.

In this paper we focus on thermal analysis of a selection of members of the Fe–Cu–Ag system. This work complements an earlier report on the structural and magnetic properties of the system as determined from x-ray diffraction and Mössbauer spectroscopy experiments [5]. Analysis of the magnetoresistive properties of these alloys is in progress, and will be reported separately in due course.

2. Experimental procedure

2.1. Sample preparation and compositional analysis

Elemental Fe and Ag powders were purchased from Aldrich Chemical Company and elemental Cu powder was purchased from Strem Chemicals Incorporated, and used as supplied. All were more than 99.9% pure. The suppliers were able to provide limited information on the pre-history of these powders as follows. The Fe powder (reference 26,795-3) had grains of size less than 10 μm and was made by a proprietary chemical process. The Ag powder (reference 32,708-5) contained particles ranging in size from 2.0 to 3.5 μm and was made via carbonate ignition. The Cu powder (reference 29-0075) comprised spherical particles graded at -100 mesh, so typically 90% of the particles would pass through a sieve with 149 μm diameter holes, and was made via atomization.

Mechanical alloying was carried out using a Fritsch Pulverisette 7 high-energy planetary ball mill with hardened steel bowls and balls[†]. Approximately 8 g of sample was used in each case, with a ball-to-powder mass ratio of order 12 to 1. The milling disc rotation frequency was set to 600 rpm. To prevent excessive heating the mill was operated continuously for two-hour periods, interspersed with cooling down periods of one hour. In this way the mean temperature of the steel bowls and balls was kept at 40 ± 5 °C throughout. All of the samples were milled for 70 hours to ensure completion of the alloying process.

The milling bowls were sealed in nitrogen and tightly clamped to prevent oxidation. Some equivalent samples were milled in air for comparison. Metal oxides were found to be present in the air-milled samples, but were absent in those that were milled in nitrogen. It was also noted that after milling in air the milling bowl contained a partial vacuum, indicating that oxygen was absorbed and that the seal on the milling container was vacuum tight.

Seven samples were milled from starting mixes of Fe-only, Cu-only, Ag-only, equimolar Fe–Cu, Fe–Ag and Cu–Ag, and equimolar Fe–Cu–Ag. Compositional analysis was carried out on the Fe-only and equimolar Fe–Cu–Ag samples using a Hitachi S-400 scanning electron microscope with an energy-dispersive x-ray analysis attachment. Elemental atomic percentages were determined within ± 0.4 at.%. The Fe-only milled sample was found to contain 96.5 at.% Fe, with 2.3 at.% Cr as the major impurity and other metals including Ni and Mn making up the remaining 1.2 at.%. Assuming that the Cr originated from the stainless steel balls and bowls, this corresponds to the incorporation of approximately 12 at.% stainless steel into the milled product. This is rather high but not unexpected given the abrasive nature of iron powder, and represents the maximum anticipated contamination.

The equimolar Fe–Cu–Ag alloy was found to have less contamination, with 0.7 at.% Cr incorporated into the product. The Fe, Cu and Ag compositions were 35.3 at.%, 33.5 at.% and 30.4 at.% respectively, with other metals including Ni making up the remaining 0.1 at.%. Again assuming that the Cr originated in the stainless steel containers, this implies 3.7 at.% steel incorporation in the alloy. This is consistent with the excess Fe relative to Cu and Ag evident in the product. The lower overall level of contamination for the alloy compared to the Fe-only milled sample is reasonable given the more malleable nature of Cu and Ag [6][‡]. Further indication of a qualitative difference between the materials comes from the observation that the milled Fe took the form of loose fine particles whereas the milled Fe–

[†] The stainless steel was type 4301, with composition 68 at.% Fe, 19 at.% Cr, 8 at.% Ni, 2 at.% Mn, 2 at.% Si and traces of S and C.

[‡] The bulk moduli of polycrystalline Fe, Cu and Ag are 169.8, 137.8 and 103.6 GPa respectively.

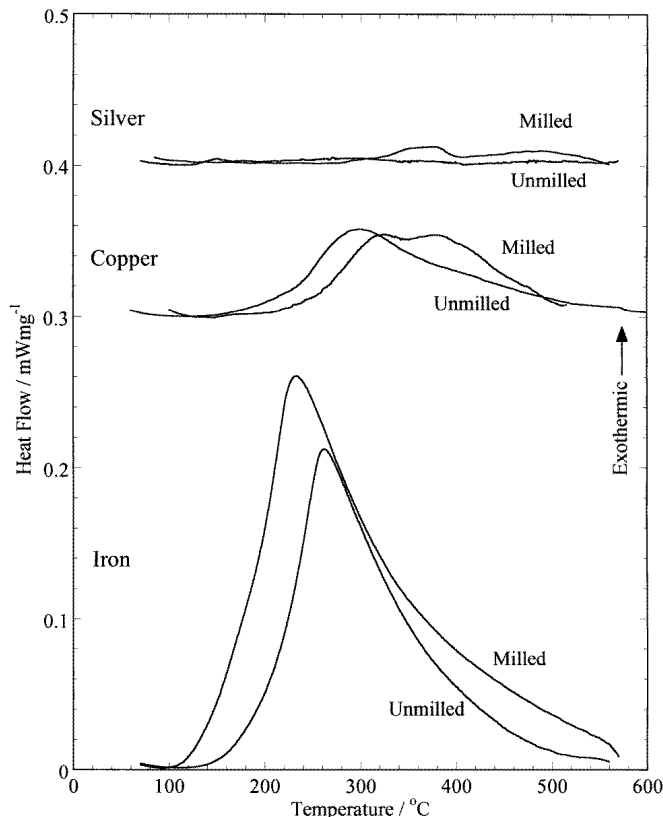


Figure 1. DSC curves for pure elemental Fe, Cu and Ag powders prior to and after mechanical alloying in a planetary ball mill operating at 600 rpm for 70 hours. For clarity, the ordinates of the curves for Cu and Ag have been offset relative to those for Fe by 0.3 mW mg^{-1} and 0.4 mW mg^{-1} respectively.

Cu–Ag formed large aggregates which tended to adhere to the surface of the milling balls.

We conclude that the samples prepared for this study contain of order 4 to 12 at.% contamination with elements from the stainless steel milling balls and bowls, with those materials containing the most Fe also having the most contamination. In the remainder of this paper we refer to the alloy samples by the compositions of the starting mixtures, namely Fe only, Cu only, Ag only, $\text{Fe}_{50}\text{Cu}_{50}$, $\text{Fe}_{50}\text{Ag}_{50}$, $\text{Cu}_{50}\text{Ag}_{50}$ and equimolar Fe–Cu–Ag, in keeping with the notation in our previous work [5].

2.2. Thermal and structural analysis

Differential scanning calorimetry (DSC) measurements were made with a Shimadzu DSC-50 calibrated against In and Zn standards, at a heating rate of $20 \text{ }^\circ\text{C min}^{-1}$. Samples of $\sim 20 \text{ mg}$ mass were placed in open platinum pans. The atmosphere above the samples was moderated with a nitrogen flow of 20 ml min^{-1} , which was known to reduce, but not eliminate completely, the likelihood of oxidation in metal samples.

Structural analysis was carried out using a Philips X-Pert x-ray diffractometer in θ – θ reflection geometry with Mo $\text{K}\alpha$ radiation, with $\lambda = 0.7107 \text{ \AA}$. ^{57}Fe Mössbauer spectra

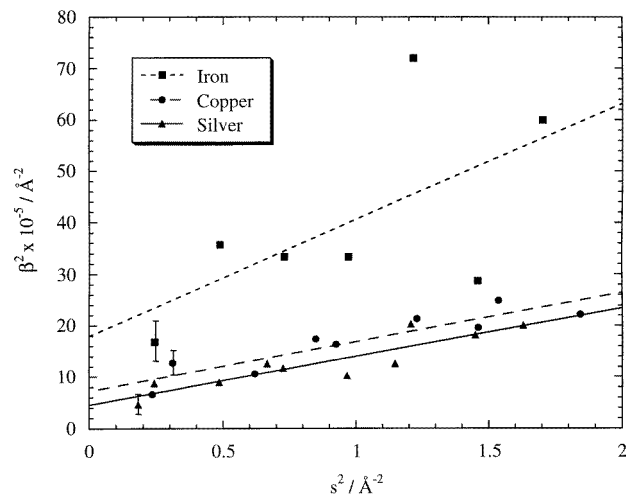


Figure 2. X-ray diffraction linewidth data analysed to distinguish between line broadening due to lattice strain and line broadening due to small particle size, as discussed in the text.

were collected with a Wissel MA-260S constant-acceleration transducer. A triangular drive waveform was used, and spectra were folded to remove base-line curvature. Calibration was carried out with respect to α -iron at room temperature.

3. Results and discussion

3.1. Pure Fe, Cu and Ag

DSC scans of the pure elemental Fe, Cu and Ag powders, before and after mechanical alloying, are shown in figure 1. Somewhat surprisingly the unmilled Fe and Cu powders contain stored energies comparable to those of their milled forms. This is presumably a reflection of the different preparation histories and/or particle size of the powders: the relatively small Ag particles prepared by carbonate ignition contain little energy, whereas the larger Fe and Cu particles prepared by chemical and atomization routes have more. Comparing the DSC scans for the milled powders shows that Fe has substantial stored energy whereas Cu and Ag both have relatively little. Assuming that the exotherms are due to energy introduced by the milling process in the form of lattice defects, distortions and dislocations, this implies that the milled Fe contains more lattice strain than either the milled Cu or the milled Ag.

This hypothesis was tested by analysing the x-ray diffraction data for the samples. These data, which have been published previously [5], show substantial line broadening due to a reduction in crystallite size and/or an increase in lattice strain. In order to disentangle these two effects we adopt a reciprocal-space formalism [7, 8]. The strains e in the crystal lattice give rise to a line broadening $\beta_e = 2.5\langle e^2 \rangle^{1/2}s$, where $s = 2 \sin \Theta / \lambda$, Θ is the Bragg angle and λ is the x-ray wavelength. The line broadening due to particle size is $\beta_D = 1/D$ where D is the mean crystallite size. Assuming Gaussian line profiles for the strain and size contributions, the total observed line broadening β obeys the relation $\beta^2 = \beta_e^2 + \beta_D^2$ [7]. By plotting β^2 as a function of s^2 we therefore obtain a measure of the rms strain $\langle e^2 \rangle^{1/2}$ from the slope, and a measure of D from the ordinate intercept.

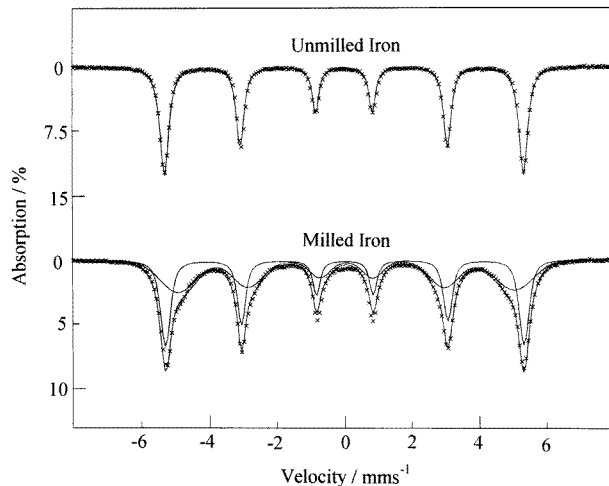


Figure 3. Room temperature Mössbauer spectra of elemental Fe powder prior to and after mechanical alloying.

From the data shown in figure 2 it is clear that the lattice strain contribution is larger for the milled Fe powders than for either the Cu or Ag powders. The calculated rms strains are $0.60 \pm 0.15\%$ for Fe and $0.39 \pm 0.05\%$ for both Cu and Ag; and the particle sizes are 7.5 ± 1.5 nm, 11.8 ± 2.5 nm and 14.8 ± 2.5 nm for Fe, Cu and Ag respectively. These results are consistent with those previously reported for a series of fcc metals, where it was shown that the lowest final particle size and highest lattice strain were found in the elements with the highest melting point and bulk modulus [6].

For further information on the origin of the lattice strain in the milled Fe powder, ^{57}Fe Mössbauer spectra of milled and unmilled powders were recorded at room temperature (figure 3). The unmilled sample shows the usual six-line hyperfine spectrum of bcc α -Fe, with the ^{57}Fe nuclei sitting in an environment that produces a nuclear hyperfine field B_{hf} of 33.0 T. Significant line broadening is apparent in the peaks of the milled sample. This spectrum has been fitted as two components, one due to Fe atoms in a relatively undisturbed α -Fe environment, and a second sextet with $B_{hf} \approx 31.1$ T, accounting for 52% of the total spectral area, due to Fe atoms in a disturbed environment.

There are several contributing factors that might give rise to the broadened Mössbauer sextet, such as gaseous contamination, alloying with Cr impurities from the stainless steel milling containers, and local distortions at grain boundaries. Gaseous contamination deserves consideration, as previous studies have shown effects such as the formation of iron nitrides [9] or the development of a body-centred tetragonal Fe phase [10]. However, in both these studies very-high-energy specialized ball mills were used, and large amounts of nitrogen were available during processing, with the milling containers being respectively filled under high pressure or continuously flushed with the gas. In our case the containers were sealed at room pressure, so comparatively limited contamination could be expected. Further observations eliminated the possibility that gaseous absorption is the cause of the broadened Mössbauer component: (i) the same component was present even when the Fe was milled in argon rather than nitrogen, ruling out nitridation, and (ii) the relative spectral area of the component increased continuously with milling time, whereas if it were due to gas absorption it would be expected to approach a limit as the supply of gas was depleted.

Alloying with impurities is a likely candidate, since we know that 2.3 at.% Cr is present in the milled sample. Fe and Cr are miscible, so it is to be expected that they will alloy as a random substitutional solid solution. It has been shown in studies of forged ingots that the effect of the addition of small quantities of Cr to Fe is to generate additional magnetic components in the Mössbauer spectrum with a lower hyperfine field than that of α -Fe [11]. The mean hyperfine field was reported to fall to 32.5 T for 2.18 at.% Cr, 32.2 T for 3.89 at.% Cr and to 31.9 T for 4.85 at.% Cr [11]. To test whether Cr impurities were indeed the origin of the broad sextet, samples of pure Fe and $\text{Fe}_{97}\text{Cr}_3$ were prepared using Cr-free milling containers made of Syalon, Si_3N_4 , which were expected to give similar but not identical products[†]. It was found that the Syalon-milled Fe showed a single-sextet Mössbauer spectrum corresponding to α -Fe, while the Syalon-milled $\text{Fe}_{97}\text{Cr}_3$ alloy showed a second broadened sextet with $B_{hf} \approx 31.4$ T and area $\sim 60\%$, so the mean hyperfine field was ~ 32.0 T. These results are both consistent with the broadened sextet in the stainless-steel-milled Fe being due to Cr alloying. It may also be noted that the main disturbance associated with the substitution of Cr for Fe on the α -Fe lattice will be magnetic rather than structural, given the similarity in the metallic radii of Fe and Cr, which are 1.22 Å and 1.25 Å respectively.

The Mössbauer contribution of those Fe atoms at grain boundaries is not known *a priori*, although it is clear from the x-ray data that some significant lattice strain is present in the milled material, and that these strains will most likely be greatest at the grain boundaries. This is perhaps the origin of a larger than usual distribution in hyperfine fields for the α -Fe component in the milled Fe spectrum, $\Delta B_{hf} \approx 0.6$ T, compared to ~ 0.2 T for the unmilled α -Fe powder.

3.2. Binary alloys

In earlier work, the structural properties of the three different binary alloy series were established [5]. In mechanically alloyed $\text{Cu}_{100-x}\text{Ag}_x$ a single-phase fcc solid solution results, irrespective of starting composition. In $\text{Fe}_{100-x}\text{Cu}_x$ single-phase solid solutions are formed: fcc for $x > 40$ and bcc for $x < 20$. In the intermediate range, a mixed phase results. In $\text{Fe}_{100-x}\text{Ag}_x$ no alloying occurs, and a microcrystalline mixture of elemental Fe and Ag particles results.

DSC curves for three binary alloys are shown in figure 4: the fcc solid solutions $\text{Cu}_{50}\text{Ag}_{50}$ and $\text{Fe}_{50}\text{Cu}_{50}$, and the granular mixture $\text{Fe}_{50}\text{Ag}_{50}$. A series of broad exothermic peaks are evident between 130 °C and 540 °C for $\text{Cu}_{50}\text{Ag}_{50}$, while $\text{Fe}_{50}\text{Cu}_{50}$ shows three main peaks at approximately 270 °C, 380 °C and 460 °C. The main peaks for the granular $\text{Fe}_{50}\text{Ag}_{50}$ alloy are at higher temperatures, of order 470 °C and 520 °C.

Given the known microstructures of the three alloys, we may surmise that the relative absence of any exotherms below 400 °C for $\text{Fe}_{50}\text{Ag}_{50}$ is due to its granular state. In $\text{Cu}_{50}\text{Ag}_{50}$ and $\text{Fe}_{50}\text{Cu}_{50}$ energy is released on heating due to both lattice recovery and decomposition to the respective elements. In contrast, $\text{Fe}_{50}\text{Ag}_{50}$ is a granular mixture and is intrinsically phase segregated, so only lattice recovery processes occur on heating. We infer that decomposition accounts for the lower-temperature peaks in the DSC thermograms, with recrystallization and grain growth of the separate elemental particles giving the higher-temperature features. The decomposition process is gradual, as is evident from by the broad nature of the DSC exotherms. A possible and likely transformation route is spinodal decomposition, although an equally slow phase separation via nucleation and growth cannot

[†] Syalon has a lower density than the stainless steel used in this study, 3.24 g cm^{-3} compared to 7.9 g cm^{-3} , and therefore does not possess the same grinding efficiency.

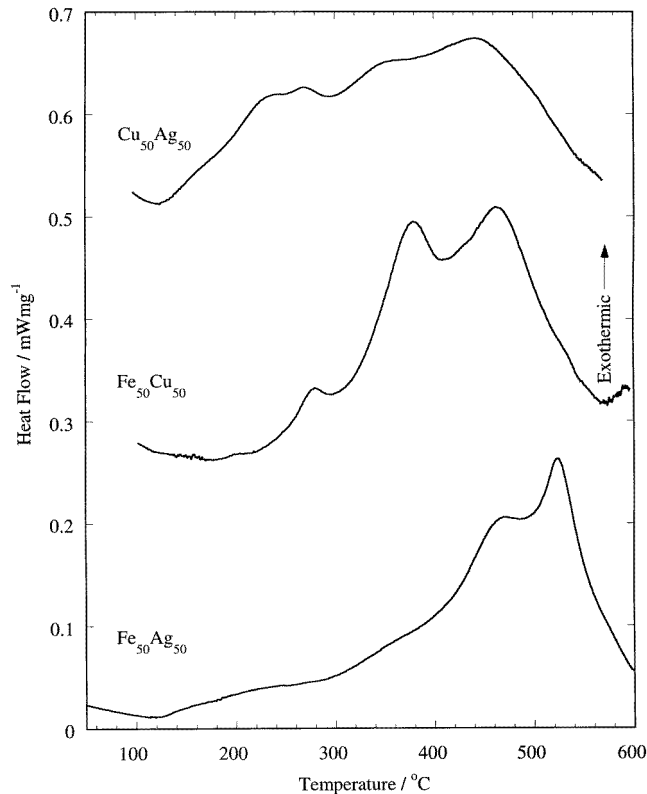


Figure 4. DSC curves for the mechanically alloyed fcc solid solutions $\text{Cu}_{50}\text{Ag}_{50}$ and $\text{Fe}_{50}\text{Cu}_{50}$, and the granular mixture $\text{Fe}_{50}\text{Ag}_{50}$. For clarity, the ordinates of the curves for $\text{Cu}_{50}\text{Ag}_{50}$ and $\text{Fe}_{50}\text{Cu}_{50}$ have been offset relative to those for $\text{Fe}_{50}\text{Ag}_{50}$ by 0.27 mW mg^{-1} and 0.52 mW mg^{-1} respectively.

be ruled out.

As a more detailed investigation, x-ray diffraction was used to examine the DSC residues of the three binary materials. Samples were heated to intermediate temperatures of between 150°C and 300°C , as well as to 600°C , and then rapidly quenched to room temperature by exposing them to air and placing them in contact with a copper heat sink. This confirmed the analysis of the thermal data in terms of phase separation followed by recrystallization. Additionally, comparisons between the results for $\text{Cu}_{50}\text{Ag}_{50}$ and $\text{Fe}_{50}\text{Cu}_{50}$ demonstrated that decomposition commenced in the former material at a significantly lower temperature than in the latter. The sample residue of $\text{Cu}_{50}\text{Ag}_{50}$ taken at 200°C comprised separate Cu and Ag crystallites whereas that of $\text{Fe}_{50}\text{Cu}_{50}$ was an unchanged solid solution alloy. This is consistent with the DSC thermograms, where exothermic processes began at 100°C for $\text{Cu}_{50}\text{Ag}_{50}$ but not until 250°C for $\text{Fe}_{50}\text{Cu}_{50}$.

In unpublished work we have found that this lack of thermal stability occurs throughout the Cu–Ag system. It is likely that it results from the 13% mismatch in atomic radii of Cu and Ag (compared to 1.5% mismatch for Fe and Cu) which leads to substantial strain in the solid solution lattice, as is apparent from the broadening of the x-ray lines of Cu–Ag [5]. This is particularly so for $\text{Cu}_{50}\text{Ag}_{50}$ which is the most distorted as a result of the presence of equal proportions of large silver and small copper atoms. The total energy released on

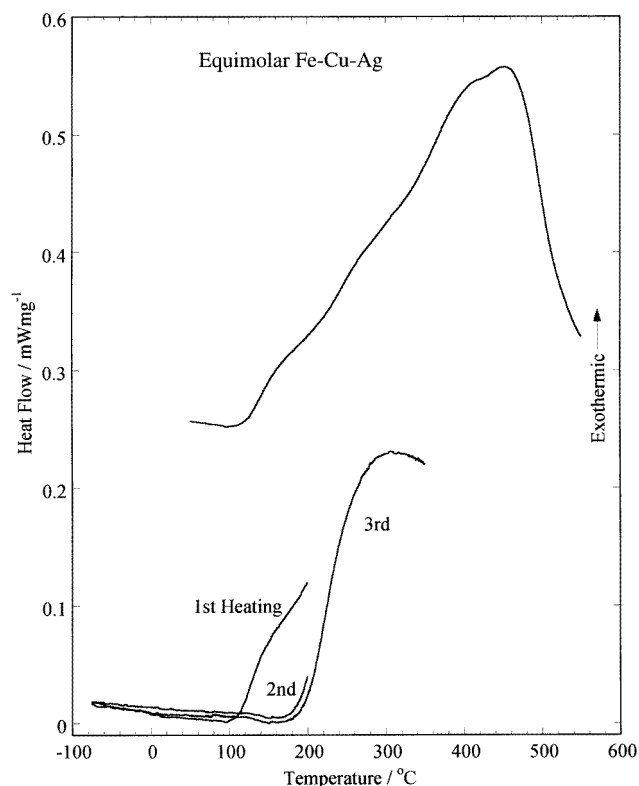


Figure 5. Upper: the DSC curve for mechanically alloyed equimolar Fe–Cu–Ag. Lower: DSC curves following thermal treatment: first and second heatings from room temperature to 180 °C, then quenching to room temperature; third heating to 350 °C. Note that for clarity the ordinate of the second heating curve is offset by 0.01 mW mg⁻¹ relative to that for the third heating curve, as otherwise the curves overlap and are indistinguishable.

heating, evident as the area under the DSC thermogram, is also greatest for the equimolar alloy.

3.3. Ternary alloys

The ternary Fe–Cu–Ag system encompasses single-phase, mixed-phase and structurally disordered alloys, depending on composition [5]. Fcc, paramagnetic ternary alloys form in both the Ag-rich and Cu-rich corners of the phase diagram. In the Fe-rich corner, mixed phases of bcc Fe–Cu alloy and fcc Ag particles form. Increasing disorder occurs in the central portion of the phase diagram, with the alloys Fe₃₀Cu₃₀Ag₄₀, Fe₃₀Cu₄₀Ag₃₀, Fe₂₀Cu₄₀Ag₄₀ and equimolar Fe–Cu–Ag all exhibiting highly broadened x-ray diffraction lines, and Mössbauer spectra that are indistinguishable from those of melt-spun Fe-based amorphous alloys.

The DSC curve for the equimolar Fe–Cu–Ag alloy in figure 5 shows a gradual response, starting at around 100 °C, rising to a maximum near 480 °C, and returning towards zero at higher temperatures. This is quite different from the reported DSC curves for amorphous Fe–Cu–Ag alloys made by sputtering, where a sharp peak near 130 °C was taken as evidence for atomic scale amorphicity, with a sudden onset of crystallization that was uniform throughout

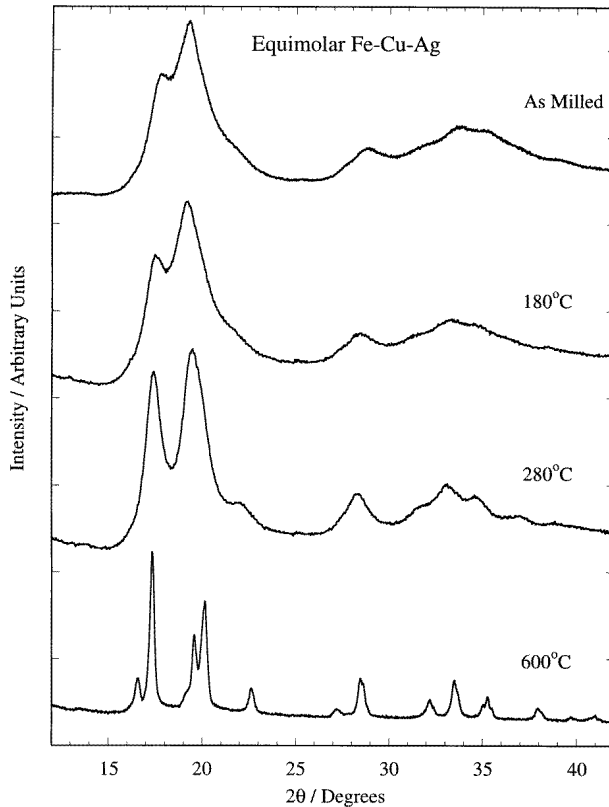


Figure 6. X-ray diffraction patterns of mechanically alloyed equimolar Fe–Cu–Ag as milled, and after having been heated at $20\text{ }^{\circ}\text{C min}^{-1}$ to 180, 280 and $600\text{ }^{\circ}\text{C}$, and then quenched to room temperature.

the sample [1, 2].

To understand the differences in the DSC curves for the sputtered and mechanically alloyed materials it is important to distinguish the crystallization of an amorphous phase from its decomposition and/or phase segregation. On heating the sputtered Fe–Cu–Ag samples to $130\text{ }^{\circ}\text{C}$ the originally amorphous material crystallized, forming an fcc phase. Further heating was needed before this metastable alloy phase segregated into the three separate elements. DSC of the mechanically alloyed Fe–Cu–Ag showed no equivalent crystallization peak. Rather, the broad featureless trace suggests that, on heating, the alloy almost immediately begins to undergo decomposition with the resulting growth of separate Fe, Cu and Ag crystallites.

To test this hypothesis, DSC scans were recorded on thermal cycling of the sample, as shown in figure 5. First the sample was heated to $195\text{ }^{\circ}\text{C}$ and quenched to room temperature. On a second heating to $195\text{ }^{\circ}\text{C}$ the exothermic signal did not appear until about $180\text{ }^{\circ}\text{C}$, implying that the heat evolved from $100\text{ }^{\circ}\text{C}$ to $195\text{ }^{\circ}\text{C}$ in the first heating run had indeed been due to the formation of crystallites. For the second heating, where initial crystallites already exist, the exotherm onset shifted to $180\text{ }^{\circ}\text{C}$. On third heating the onset of crystallization was again near $180\text{ }^{\circ}\text{C}$. Continued heating to $350\text{ }^{\circ}\text{C}$ brought the DSC signal back towards its original value.

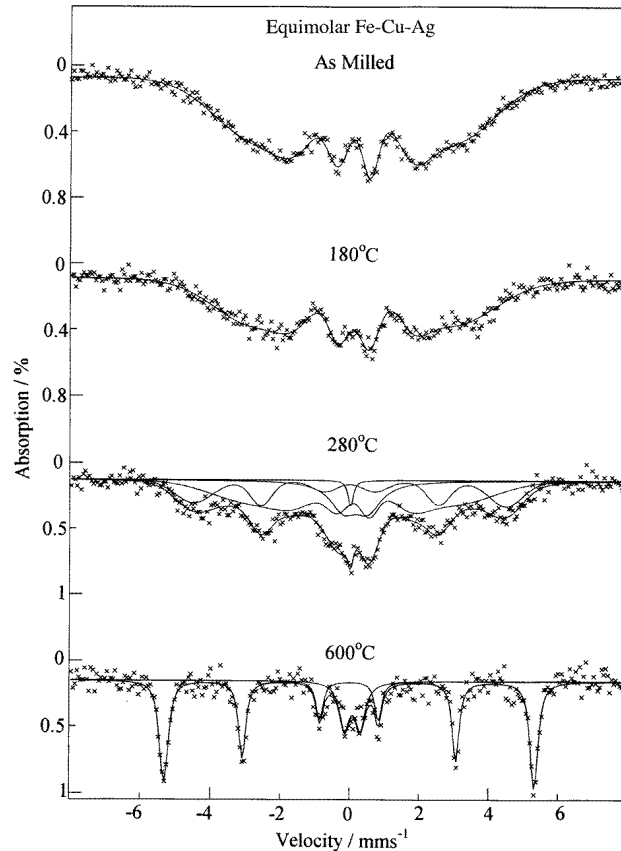


Figure 7. Room temperature Mössbauer spectra of mechanically alloyed equimolar Fe–Cu–Ag as milled, and after having been heated at $20\text{ }^{\circ}\text{C min}^{-1}$ to $180\text{ }^{\circ}\text{C}$, $280\text{ }^{\circ}\text{C}$ and $600\text{ }^{\circ}\text{C}$, and then quenched to room temperature.

Further evidence of the gradual segregation process was obtained by recording x-ray diffraction and Mössbauer data on the DSC residues of samples that were heated to $180\text{ }^{\circ}\text{C}$ and $280\text{ }^{\circ}\text{C}$ and then quenched to room temperature, as well as for samples that were subject to the complete heating cycle from room temperature to $600\text{ }^{\circ}\text{C}$. The x-ray data in figure 6 show that heating to $180\text{ }^{\circ}\text{C}$ produces only a very small change in the structure, most evident in the slightly more separated lines at 2θ -values of 18° and 20° . The sample heated to $280\text{ }^{\circ}\text{C}$ shows more decomposition, with the positions of the evolving peaks being consistent with those of elemental Fe, Cu and Ag. Even so, it is not possible to resolve the elements individually, as the peak widths are large, either due to the small crystallite sizes and strain effects, or due to the continued presence of partially alloyed particles. The x-ray pattern of the $600\text{ }^{\circ}\text{C}$ residue shows sharp peaks corresponding to fully polycrystalline and segregated Fe, Cu and Ag phases, plus a small component due to copper oxide. The latter is most likely to be due to air contamination of the calorimeter.

Corresponding ^{57}Fe Mössbauer spectra are shown in figure 7. The as-milled sample has an extremely broad spectrum, with no sign of sharp absorption peaks due to any crystalline phase. The spectrum of the $180\text{ }^{\circ}\text{C}$ quenched sample is only slightly different, consistent with the small change observed in the x-ray data. The spectrum of the $280\text{ }^{\circ}\text{C}$ quenched

sample shows that decomposition and crystallization has commenced, but is not complete. Roughly half of the Fe atoms are still in the highly disordered environment of the as-milled state, while the remainder are in a more crystalline state, evident from the relatively narrow lines of the new magnetic sextet evident in the spectrum. The magnetic hyperfine field of this component is approximately 27.6 T, which is less than the 33.1 T that is characteristic of pure α -Fe, indicating residual alloying. There is also an additional paramagnetic component indicating the presence of isolated Fe atoms within the bulk of another element. The spectrum of the 600 °C residue shows the fully crystalline pattern of bcc Fe, plus a small paramagnetic doublet, probably due to ferric ions in an iron oxide.

The Mössbauer data provides some evidence regarding the nature of the phase segregation process. The 280 °C spectrum in particular is instructive, since even the more crystalline state shows residual alloying rather than the characteristic spectrum of pure α -Fe. The latter is what might be expected from a nucleation and growth mechanism, while the former is consistent with a spinodal decomposition process.

4. Conclusions

Thermal analysis of Fe–Cu–Ag alloys prepared by high-energy ball milling has provided valuable information on the metastability of the alloys, complementing an earlier study of the structure and magnetic properties by x-ray diffraction and Mössbauer spectroscopy. DSC and x-ray data on the milled pure elements show that Fe has a greater propensity to sustain and retain lattice distortion than either Cu or Ag. Mössbauer data on the milled Fe sample showed evidence of a disturbed magnetic environment for some of the Fe atoms, identified as due to the presence of 2.3 at.% Cr atoms from the stainless steel milling containers. In the binary alloys, the absence of low-temperature DSC exotherms for Fe₅₀Ag₅₀ confirms the high degree of phase segregation in this granular alloy, compared to the fcc solid solutions Cu₅₀Ag₅₀ and Fe₅₀Cu₅₀. X-ray studies of DSC residues at intermediate temperatures were able to confirm the assignment of those DSC exotherms below 400 °C to the decomposition of the alloy into its constituent elements, and those at higher temperatures to recrystallization and grain growth. For the equimolar Fe–Cu–Ag alloy, DSC curves and successive heat treatments show that a highly disordered state is present, but with residual crystallinity on a very fine scale. Heating allows the decomposition of this metastable state into polycrystalline and segregated Fe, Cu and Ag. This is confirmed by x-ray and Mössbauer data on samples heated and quenched at intermediate temperatures.

We conclude that in contrast to that produced by sputter deposition, the equimolar Fe–Cu–Ag material produced by high-energy ball milling is not amorphous in the strict sense, but rather it is a highly disordered and probably nanocrystalline state. It is also clear that on heating the binary and ternary equimolar alloys there is a gradual decomposition of the alloy into its constituent elements at temperatures below about 400 °C, followed by crystallite and grain growth at higher temperatures. This latter observation may be important for controlling the microstructural properties of these and similar systems, such as in giant-magneto-resistive applications where granularity, phase segregation and the degree of grain-to-matrix admixture contribute to the performance of the material.

Acknowledgments

The Mössbauer and DSC data were collected under the auspices of the University of London Intercollegiate Research Service.

References

- [1] Sumiyama K, Nishi K and Suzuki K 1991 Amorphous structure of the immiscible $\text{Fe}_{1-y}(\text{Cu}_{1-x}\text{Ag}_x)_y$ alloy system *J. Phys.: Condens. Matter* **3** 9859–69
- [2] Sumiyama K, Yoshimoto K and Shiga M 1993 Hierarchy of non-equilibrium phases in the immiscible Fe–Cu–Ag alloy system *Acta Metall. Mater.* **41** 2487–95
- [3] Wang J Q, Xiong P and Xiao G 1993 Investigation of giant magnetoresistance in concentrated and nanostructured alloys *Phys. Rev. B* **47** 8341–4
- [4] Makhlof S A, Sumiyama K, Wakoh K, Suzuki K, Takanashi K and Fujimori H 1993 Giant magnetoresistance of Fe-cluster-dispersed Ag films *J. Magn. Magn. Mater.* **126** 485–8
- [5] Cohen N S, Ahlswede E, Wicks J D and Pankhurst Q A 1997 Investigation of the ternary phase diagram of mechanically alloyed FeCuAg *J. Phys.: Condens. Matter* **9** 3259–76
- [6] Eckert J, Holzer J C, Krill C E and Johnson W L 1992 Structural and thermodynamic properties of nanocrystalline fcc metals prepared by mechanical attrition *J. Mater. Res.* **7** 1751–61
- [7] Klug H P and Alexander L 1974 *X-ray Diffraction Procedures for Polycrystalline and Amorphous Materials* (New York: Wiley)
- [8] Oleszak D and Shingu P H 1996 Nanocrystalline metals prepared by low energy ball milling *J. Appl. Phys.* **79** 2975–80
- [9] Calka A, Nikolov J I and Williams J S 1996 Formation, structure and stability of iron nitrides made by reactive ball milling *Mater. Sci. Forum* **225** 527–32
- [10] Cook D C, Kim T H and Rawers J C 1996 Microstructural development of iron powder during Attritor ball-milling in nitrogen *Mater. Sci. Forum* **225** 533–8
- [11] Dubiel S M, Zukrowski J, Korecki J and Krop K 1975 The effect of neighbouring chromium atoms on hyperfine magnetic field at ^{57}Fe nuclei in Fe–Cr alloys *Acta Phys. Pol. A* **47** 199–205